


ORIGINAL ARTICLE

Cytoplasmic HDAC4 recovers synaptic function in the 3×Tg mouse model of Alzheimer's disease

Claudia Colussi^{1,3}  | Giuseppe Aceto^{2,3} | Cristian Ripoli^{2,3} | Alessia Bertozzi¹ |
Domenica Donatella Li Puma^{2,3} | Elena Paccosi¹ | Marcello D'Ascenzo^{2,3} |
Claudio Grassi^{2,3}

¹Department of Engineering, Istituto di Analisi dei Sistemi ed Informatica 'Antonio Ruberti', National Research Council, Rome, Italy

²Department of Neuroscience, Università Cattolica del Sacro Cuore, Rome, Italy

³Fondazione Policlinico Universitario Agostino Gemelli IRCCS, Rome, Italy

Correspondence

Claudia Colussi, Department of Engineering, Istituto di Analisi dei Sistemi ed Informatica 'Antonio Ruberti', National Research Council, Via dei Taurini 19, 00185 Rome, Italy.
Email: claudia.colussi@cnr.it

Funding information

Fondazione Policlinico Universitario Agostino Gemelli IRCCS; Alzheimer's Association, Grant/Award Number: 19 614919

Abstract

Aims: Early dysfunction in Alzheimer's disease (AD) is characterised by alterations of synapse structure and function leading to dysmorphic neurites, decreased spine density, impaired synaptic plasticity and cognitive deficits. The class II member HDAC4, which recently emerged as a crucial factor in shaping synaptic plasticity and memory, was found to be altered in AD. We investigated how the modulation of HDAC4 may contribute to counteracting AD pathogenesis.

Methods: Using a cytoplasmic HDAC4 mutant (HDAC4^{SD}), we studied the recovery of synaptic function in hippocampal tissue and primary neurons from the triple-transgenic mouse model of AD (3×Tg-AD).

Results: Here, we report that in wild-type mice, HDAC4 is localised at synapses and interacts with postsynaptic proteins, whereas in the 3×Tg-AD, it undergoes nuclear import, reducing its interaction with synaptic proteins. Of note, HDAC4 delocalisation was induced by both amyloid-β and tau accumulation. Overexpression of the HDAC4^{SD} mutant in CA1 pyramidal neurons of organotypic hippocampal slices obtained from 3×Tg-AD mice increased dendritic length and promoted the enrichment of N-cadherin, GluA1, PSD95 and CaMKII proteins at the synaptic level compared with AD neurons transfected with the empty vector. Moreover, HDAC4 overexpression recovered the level of SUMO2/3ylation of PSD95 in AD hippocampal tissue, and in AD organotypic hippocampal slices, the HDAC4^{SD} rescued spine density and synaptic transmission.

Conclusions: These results highlight a new role of cytoplasmic HDAC4 in providing a structural and enzymatic regulation of postsynaptic proteins. Our findings suggest that controlling HDAC4 localisation may represent a promising strategy to rescue synaptic function in AD, potentially leading to memory improvement.

KEYWORDS

Alzheimer's disease, histone deacetylases, neuropathology, SUMOylation, synapse

This is an open access article under the terms of the [Creative Commons Attribution-NonCommercial](https://creativecommons.org/licenses/by-nc/4.0/) License, which permits use, distribution and reproduction in any medium, provided the original work is properly cited and is not used for commercial purposes.

© 2022 The Authors. *Neuropathology and Applied Neurobiology* published by John Wiley & Sons Ltd on behalf of British Neuropathological Society.

INTRODUCTION

Alzheimer's disease (AD) is a neurodegenerative pathology that leads progressively to an irreversible decline of cognitive function [1]. Less than 5% of AD cases manifest an early onset with either sporadic or genetic origin, caused by mutations in the amyloid precursor protein (APP), presenilin-1 (PSEN1) and presenilin-2 (PSEN2) genes [2]. The majority of AD patients, instead, present with late-onset AD that is sporadic and determined by a number of environmental and genetic risk factors [3]. Both AD forms are characterised by the accumulation of fibrillar aggregates of hyperphosphorylated tau [4] and amyloid- β (A β) proteins, derived by aberrant APP processing [5], which, especially in the oligomeric soluble form, exerts detrimental effects on synapse structure and function causing dysmorphic neurites, decrease in spine density, reduced synaptic plasticity and memory impairment [6]. Of note, synapse dysfunction is considered one of the earliest events in AD that strongly correlates with disease severity. Accordingly, targeting synaptic proteins and their regulators could be a valuable therapeutic option to prevent and/or slow the progression of AD.

Histone deacetylases (HDACs) regulate protein function by deacetylating target lysines. Removal of acetyl groups from histone proteins induces chromatin condensation and gene repression, whereas modification of non-histone proteins is a key event for their function and regulation of cellular signalling pathways [7]. Mammalian HDACs are grouped into four different classes based on their structure and function as follows: class I (HDAC1, HDAC2, HDAC3 and HDAC8), class II (IIa: HDAC4, HDAC5, HDAC7 and HDAC9; IIb: HDAC6 and HDAC10), class III (SIRT1–SIRT7) and class IV (HDAC11). In contrast to class I HDACs, which show nuclear localisation, class II HDACs exhibit nucleocytoplasmic shuttling, which is dynamic and phosphorylation dependent [8]. Specifically, the activity of *N*-methyl-D-aspartate (NMDA) receptors induces activation of Ca²⁺/calmodulin-dependent protein kinase II (CaMKII) that regulates class II nuclear export by phosphorylation at serine 632 and 246 in the brain [9]. On the contrary, dephosphorylation promotes nuclear accumulation and repression of target genes [10].

Several works have highlighted the key role of HDAC4, a class IIa member, in neuronal function [11–13]. Under physiological conditions, phosphorylation of HDAC4 by CaMKII maintains HDAC4 in the cytoplasm preventing its nuclear accumulation [13]. HDAC4 nuclear import is implicated in the control of activity-dependent transcriptional programmes by transient repression of early response genes, such as *Fos* and *Arc* [14]. However, constitutive nuclear gain-of-function HDAC4 mutant showed repression of many genes belonging to presynaptic and postsynaptic proteins, α -amino-3-hydroxy-5-methyl-4-isoxazole propionic acid (AMPA) receptors, scaffolds and intracellular molecules implicated in plasticity and memory [13], suggesting that prolonged pathological HDAC4 nuclear localisation may contribute to neurodegeneration. Along this line, HDAC4 nuclear import has been associated with cognitive impairment in neurodegenerative diseases and in mental disorders [15–17] including

Key Points

- HDAC4 localises at dendritic spines and interacts with postsynaptic proteins.
- In AD mice, HDAC4 interaction with synaptic proteins is reduced.
- Overexpression of a cytoplasmically restricted HDAC4 mutant regulates synaptic protein enrichment by triggering post-translational modifications and providing a scaffolding platform.
- Overexpression of a cytoplasmically restricted HDAC4 mutant recovers dendritic spine density and neuronal function.
- Strategies aimed at restoring the cytoplasmic role of HDAC4 may represent a new therapeutic approach.

AD where HDAC4 nuclear accumulation has been observed in both genetic and sporadic AD mouse models [18, 19].

Conversely, other studies have shown that conditional brain-specific HDAC4 deletion determines impairment in learning and memory as well as in long-term synaptic plasticity [12] indicating a positive functional role of HDAC4 in neurons. These results possibly underline the complex mechanism of action of HDAC4 that may rely on distinct and opposite cytoplasmic and nuclear functions, which are to date not completely understood.

In the nucleus, HDAC4 exhibits low deacetylase activity [20]; thus, it represses target genes not only by deacetylating histones but also by deacetylase-independent functions interacting with HDAC3 and HDAC5 and modulating the activity of co-repressors and transcription factors [21].

In contrast to its nuclear function, the cytoplasmic function of HDAC4 has not been characterised yet. Indeed, HDAC4 in neurons is mainly cytoplasmic with a pool present at dendritic shafts and spines, but which is of unknown function [22]. However, whether loss of specific HDAC4 cytoplasmic functions may contribute to synaptic dysfunction in AD is still unknown.

Accumulating evidence indicates that the positive effect of HDAC4 on memory formation [12] might not involve deacetylase activity, but that it depends on the ability of HDAC4 to regulate other post-translational modifications (PTMs) such as SUMOylation [23]. Three different Small Ubiquitin-like Modifier (SUMO) proteins (SUMO1, SUMO2 and SUMO3) can be reversibly conjugated to lysine residues of target proteins by a sequential enzymatic cascade including SUMO activation, transfer and conjugation involving Aos1/Uba2 enzyme (E1), the UBC9 enzyme (E2) and a SUMO ligase (E3), respectively [24]. SUMOylation of target proteins regulates stability, activity, subcellular localisation and protein–protein interactions [25]. Many synaptic proteins, receptors and ion channels are SUMO targets as well as other important regulators of neuronal function, whose

alteration is associated with synaptopathies [26]. Of note, the global pattern of SUMOylated proteins in mouse models of AD is altered, with increased or decreased levels of SUMO1- or SUMO2/3-modified proteins, respectively [27]. So far, the potential role of HDAC4 in the changes of synaptic protein SUMOylation in AD is unknown.

Here, we report that HDAC4 cytoplasmic localisation and interaction with postsynaptic proteins are altered in the 3×Tg-AD mice. Aβ and tau were found to contribute, at least in part, to HDAC4 mislocalisation. Remarkably, we show that the expression of a cytoplasmically restricted HDAC4 mutant recovers synaptic protein localisation, spine density and synaptic transmission in the AD mouse model by deacetylase-independent function. Our findings point to HDAC4 as a potential new therapeutic tool for synapse function preservation.

MATERIALS AND METHODS

Animal model

3×Tg-AD (B6;129-Psen^{tm1Mpm}Tg/APPSwe, tauP301L/1Lfa/Mmjax) mice, expressing APP, PSEN and tau mutated proteins, were used as an animal model of AD. In this study, 3×Tg-AD adult (7- to 8-month-old) mice, 4-day-old pups and E18 embryos were compared with age-matched wild-type (WT) control mice (B6129SF2/J).

Primary cultures of hippocampal neurons

Hippocampal neurons were prepared from WT and AD E18 embryos according to standard procedures [28]. After isolation of the hippocampi, tissues were incubated for 10 min at 37°C in trypsin-EDTA solution (0.025%/0.01% w/v; Gibco) in PBS and then mechanically dissociated at room temperature (RT) with a fire-polished Pasteur pipette. Cell suspensions were harvested and centrifuged at 600 g for 5 min. The pellet was resuspended in MEM (Sigma-Aldrich) containing 5% foetal bovine serum, 5% horse serum, 2 mM glutamine, 1% penicillin-streptomycin antibiotic mixture (Sigma-Aldrich) and 25 mM glucose. Cells were plated on poly-L-lysine (0.1 mg/ml; Sigma-Aldrich) pre-coated wells. The medium was changed the day after (DIV1) (differentiation medium: Neurobasal, 2% B27, 1% penicillin-streptomycin antibiotic mixture [Sigma-Aldrich] and 1 mM L-glutamine) and on Day 4 (DIV4) with glutamine-free differentiation medium. Neurons at DIV12–DIV14 prepared from WT mice were treated with Aβ₄₂ oligomers (200 nM) prepared as described in Puzzo et al. [29], tau (100 nM) or LMK-235 (40 μM) for 24 h. Control cells were treated with solvent (PBS or dimethyl sulfoxide [DMSO]).

Human recombinant tau and synthetic Aβ preparations

Recombinant human tau 4R/2N was prepared as described in Li Puma et al. [30]. Oligomerisation was achieved via the introduction

of disulphide bonds through incubation with 1 mM H₂O₂ at RT for 20 h and assessed by Western blot (WB). Oligomeric Aβ was prepared as described in Ripoli et al. [31]. Peptides were diluted to 1 mM in 1,1,1,3,3,3-hexafluoro-2-propanol, to disassemble preformed aggregates, and stored as dry films at –20°C. Protein solutions were prepared by dissolving the films at 1 mM in DMSO, sonicated for 10 min, then diluted to the final concentration in PBS and incubated for 12 h at 4°C to promote protein oligomerisation.

Cell culture and treatments

The SH-SY5Y neuroblastoma cell line was grown in DMEM/Ham's F12 medium supplemented with 10% inactivated foetal bovine serum, 1% penicillin-streptomycin antibiotic mixture (Sigma-Aldrich) and 2 mM L-glutamine (Gibco). Transient overexpression of GFP-HDAC4^{WT} or GFP-HDAC4^{SD} was achieved by transfection with PEI MAX (Polyethylenimine Hydrochloride, Polysciences) according to the manufacturer's instructions. Two days after transfection, the cells were treated with Aβ₄₂ oligomers (200 nM) or tau (100 nM) for 24 h and then fixed and processed for immunofluorescence (IF).

Organotypic hippocampal slice cultures and analysis

Hippocampal organotypic slices (350 μm) were prepared from the brain of P4 pups through a McIlwain tissue chopper as described in Renna et al. [32]. At least four pups for each preparation were used. Briefly, brains were rapidly excised and kept in ice-cold and oxygenated cutting solution (2.5 mM KCl, 25.6 mM NaHCO₃, 1.15 mM NaH₂PO₄·2H₂O, 11 mM D-glucose, 238 mM sucrose, 1 mM CaCl₂ and 5 mM MgCl₂) until slicing. Slices were plated onto semi-porous tissue culture inserts (PICMORG50, Millipore) placed in a six-well culture and cultured at a liquid-air interface in medium containing 50% MEM (Eagle's with Earle's balanced salt solution), 25% heat-inactivated horse serum, 18% HBSS, 2% B27 supplemented with 4 mM L-glutamine, 50 U penicillin-streptomycin/ml and 6 mg/ml D-glucose. The culture medium was changed on the second day in vitro (DIV2) and then every other day. Slices were cultured at 35°C in humidified air with 5% CO₂ for 2 weeks. DsRed plasmid, used to identify the transfected neurons, alone or in combination with HDAC4^{SD}-FLAG plasmid, was biolistically transfected into slices at DIV10 and DIV11 by using a Gene Gun (Bio-Rad, CA, USA). DsRed2-labelled neurons in organotypic hippocampal slice cultures were subjected to electrophysiology (see below) and spine density count. Secondary dendrites were imaged using a 100×, oil-immersion objective plus a fivefold zoom. Spine density was calculated on z stacks of three-dimensional images quantifying the number of spines per dendritic segment normalised for 1 μm. A total length of at least 2 mm was analysed for each condition.

Electrophysiology and data analysis

Patch pipettes had a resistance of 4–6 M Ω when filled with an internal solution containing (in mM) K-gluconate 145, MgCl₂ 2, HEPES 10, EGTA 0.1, Na-ATP 2.5, Na-GTP 0.25 and phosphocreatine 5, pH adjusted to 7.2 with KOH. After establishing a gigaseal, the patch was broken by applying negative pressure to achieve a whole-cell configuration. A series resistance lower than 15 M Ω was considered acceptable and monitored constantly throughout the entire recording. Neurons were held at -70 mV. Recordings were performed using a MultiClamp 700B/Digidata 1550A system (Molecular Devices, Sunnyvale, CA) and digitised at a 10,000 Hz sampling frequency. For evoked and miniature excitatory postsynaptic current (EPSC) measurements, neurons were held at -70 mV. EPSCs were elicited in the CA1 neurons by placing a bipolar concentric stimulating electrode (FHC Neural microTargeting Worldwide) in the Schaffer collateral pathway. First, the input–output relationship was assessed in order to find the maximal response amplitude. Subsequent measurements for paired-pulse facilitation (PPF) were performed using stimulation that yielded 30% of the maximal response. PPF was assessed by delivering pairs of stimuli at different interstimulus intervals (ISIs; 20, 50, 100 and 200 ms), repeated at 0.05 Hz. The electrophysiological recordings were analysed using the Clampfit 10.9 software (Molecular Devices). For miniature EPSC (mEPSC) recordings, tetrodotoxin (TTX, 0.5 μ M, Tocris) and D-(–)-2-amino-5-phosphonopentanoic acid (D-AP5, 50 μ M, Tocris) were applied to the bath to block action potential-mediated neurotransmitter release and NMDA receptors. For mEPSC analysis, a template was constructed using the ‘Event detection/create template’ function, as previously described [33], and then miniature inhibitory postsynaptic currents (mIPSCs) were detected using the ‘Event detection/template search’ function. All the waveforms detected during a single recording using template analysis were averaged, and amplitude, rise time and decay time were calculated.

Mutant generation and lentiviral production

HDAC4^{SD} constructs were generated by mutation of serine 246 and 632 to aspartic acid (D) or alanine (A) by direct site mutagenesis from the GFP-HDAC4^{WT} (Addgene 45636) or the FLAG-HDAC4^{WT} (Addgene 13821) DNA (QuikChange II system, Agilent Technologies). Mutations were verified by complete sequencing. To generate lentiviral particles for neuron transduction, the HDAC4^{SD} DNA was cloned into the ECORI/Mlu site on the third-generation lentiviral vector p-Lenti-C-GFP (OriGene). Lentiviral particles were generated by transient transfection of HEK293T with transfer plasmid (HDAC4^{SD} or the GFP control vector) and packaging plasmids (pMD2G, Addgene 12259; pRSV-Rev, Addgene 12253; pMDLg/pRRE Addgene 12251). The medium containing the particles was concentrated by ultracentrifugation (virus concentration 1×10^8 TU/ml). Neurons were infected at DIV3 (MOI 5) in differentiation medium (DIV1) plus polybrene (8 μ g/ml) for 4 h, and then the medium was changed with DIV1 and the following day with DIV4. Neurons were analysed at DIV14.

Confocal analysis

Confocal analysis was performed as previously described [34]. Cells were fixed in 4% paraformaldehyde (PFA) for 10 min, permeabilised for 10 min in 0.3% Triton X-100 in PBS and blocked by incubation in 5% BSA for 1 h. Mice were anaesthetised with a cocktail of ketamine (100 mg/ml) and xylazine (1 mg/ml) and transcardially perfused with PBS (0.1 M, pH 7.4) followed by 4% PFA. Brains were removed, post-fixed overnight at 4°C, transferred in a solution of 30% sucrose for 2 days and then frozen in OCT. Coronal brain sections were cut (40 μ m thick) with a cryostat (SLEE, Mainz, Germany) and subsequently stored at 4°C in PBS until processed for IF. Free-floating sections were subjected to antigen retrieval in citrate/EDTA buffer pH 6.2 at 50°C for 30 min and then permeabilised and blocked for 45 min at RT in 5% BSA, 3% normal goat serum and 0.5% Triton X-100 (Sigma-Aldrich) in PBS. Sections or cells were incubated overnight in primary antibodies at 4°C. The following day, sections or cells were washed in PBS and secondary antibodies were added for 1 h and 30 min at RT. After a brief rinse, nuclei were counterstained with DAPI and slides mounted with prolong gold antifade. Samples were analysed with a confocal laser scanning system (Nikon ECLIPSE Ti equipped with a 20 \times -40 \times -60 \times -100 \times objective). Confocal settings were the same for all examined samples to compare fluorescence intensities. 3D images of cells, derived from the reconstruction of the z series, were used to calculate the mean fluorescence intensity (MFI) by ImageJ software. Signals from single regions of interest were used to calculate the average values for fluorescence intensity. A minimum of three sections for each animal were analysed. Data are presented as mean values \pm standard error of the mean (SEM).

WB, immunoprecipitation (IP) and antibodies

Hippocampi were isolated from brains and used for preparation of cytosolic fractions (NE-PER Thermo Fisher) or total protein extracts by RIPA buffer (10 mM Tris-HCl [pH 7.4], 140 mM NaCl, 1% Triton X-100, 0.1% sodium deoxycholate, 0.1% SDS and 1 mM EDTA) supplemented with 1 mM PMSF and protease inhibitor mix. WB was carried out according to standard procedures, and ECL signals were acquired and analysed with the UVITEC imaging system. Optical density values of specific proteins were normalised to that of tubulin, β -actin or GAPDH, which in our experimental settings were unchanged. Results are expressed as fold change vs WT/control samples, which were considered equal to 1. Representative WBs are shown in the figures, and graphs show the mean of at least three independent experiments \pm SEM. The following antibodies were used: anti-HDAC4 (WB 1:1000, IF 1:300, polyclonal, Abcam, Ab12172), anti-phospho-S632-HDAC4 (WB 1:1000, polyclonal, Novusbio, NB-100-92689), anti-tau (WB 1:1000, monoclonal, Invitrogen, HT7), anti-H3 (WB 1:2000, polyclonal, Abcam, ab1791), anti-GAPDH (WB 1:2000, monoclonal, Abcam, ab8245), anti-GFP (WB 1:1000, polyclonal, Santa Cruz, sc-8334), anti-CaMKII

(WB 1:1000, monoclonal, Santa Cruz, sc-5306), anti-Nup50 (WB 1:1000, polyclonal, Abcam, Ab85915), anti-PSD95 (WB 1:1000, polyclonal, Cell Signaling, 3550), anti-GluR1 (WB 1:1000, monoclonal, Cell Signaling, MB2263), anti-N-cadherin (WB 1:1000, polyclonal, Abcam, Ab18203), anti-pan-14-3-3 (WB 1:1000, monoclonal, Santa Cruz), anti-phospho-Thr286-CaMKII (WB 1:1000, Santa Cruz), anti-tubulin (WB 1:4000, monoclonal, Abcam, ab7291) and anti- β -actin (WB 1:2000, polyclonal, Abcam, ab8227). Co-immunoprecipitation (co-IP) experiments were performed using 3 μ g of antibody for 400 μ g of protein extract. Ademtech's Bio-Ademeads paramagnetic bead system was used to immunoprecipitate the specific proteins. Negative controls were performed with the same amount of protein extract sample immunoprecipitated with the corresponding purified IgG (Santa Cruz). Total sample inputs were run in the WB as loading controls. In co-IP experiments, the relative association between proteins was performed according to Burckhardt et al. [35] calculating the band OD ratio between the target proteins and the bait (HDAC4).

In vitro SUMOylation assay

Samples were extracted in RIPA buffer containing 1% SDS plus a protease inhibitor mix and 50 mM *N*-ethylmaleimide (NEM) to block SUMO proteases. Lysates (500 μ g of total protein) were subjected to IP using anti-PSD95 antibody (3 μ g/sample) cross-linked to paramagnetic beads (Bio-Ademeads) overnight. The immune complexes were washed and eluted according to the manufacturer's instruction, and an equal amount of WT and AD immunoprecipitates were used in the in vitro SUMOylation assay (Abcam Ab139470). Where indicated, the GFP-HDAC4^{SD} expressed in SH-SY5Y or IgG-control purified by IP with paramagnetic beads were added to the AD sample in the in vitro SUMOylation reaction. The products of the enzymatic reaction were processed by WB (8% SDS-PAGE under non-reducing conditions) using anti-SUMO2/3 (Cytoskeleton monoclonal ASM24), anti-PSD95 (Cell Signaling polyclonal 3550) and anti-HDAC4 (Abcam polyclonal Ab12172) antibodies to detect the immunoprecipitated proteins. SUMO-RanGAP was used as a positive control of the enzymatic reaction.

A β dot blot

A β oligomers were evaluated by dot blot experiments in which 5 μ l (15 μ g of proteins) of lysate was spotted directly on the membrane. After blocking (5% milk in TBST), membranes were probed with the anti- β -amyloid (WB 1:1000, monoclonal, BioLegend, 803014-6E10). o.n. and then the signal revealed by secondary antibody and ECL reaction as in the WBs. Optical density values of the A β signal were normalised to red Ponceau staining to verify the total protein loading. Results are expressed as fold change vs WT/control samples, which were considered equal to 1.

Cellular fractioning

Neuronal cultures or brains from sacrificed mice were washed in ice-cold PBS and suspended in 10% (w/v) of 0.32 M sucrose-HEPES buffer along with protease inhibitor and homogenised with 10 up-and-down even strokes, and then the homogenates were centrifuged at 4°C for 10 min at 600 g. The pellet, containing the nuclear fraction, was washed in PBS and lysed in RIPA buffer plus 1% Triton X-100 and protease inhibitors. The supernatant was diluted 1:1 with 1.3 M sucrose-HEPES to obtain a final concentration of 0.8 M sucrose-HEPES. This suspension was further centrifuged three times at 12,000 g for 15 min at 4°C washing with HEPES buffer and discarding the supernatant each time to remove sucrose-HEPES buffer contamination. The pellet consisting of synaptosomes was suspended in RIPA buffer supplemented with protease inhibitor and PMSF along with 0.2% Triton X-100 and rotated at 4°C for 1 h to resuspend the proteins.

Statistics

SigmaPlot 14.0 software was used to calculate significance. Sample size (*n*) is indicated in the main text and represents independent experiments from different cell culture preparations or animals. A comparison of two groups was performed by *t* test for normally distributed samples or by the Mann-Whitney rank-sum test for non-normally distributed samples. Multiple comparisons were carried out by one-way analysis of variance (ANOVA) followed by the Bonferroni post hoc test for normally distributed samples. In the other cases, non-parametric tests (ANOVA on ranks followed by post hoc tests), as indicated in the text, were applied. *p* values <0.05 were considered significant in all tests. For all analyses, the observer was blind to the identity of the samples.

RESULTS

HDAC4 cytoplasmic localisation and synaptic interactions are altered in the 3 \times Tg mouse model of AD

To address the role of the HDAC4 pool specifically localised at synapses and its impact on AD pathology, we investigated HDAC4 binding partners by co-IP in cytoplasmic lysates of hippocampal tissues from WT and 3 \times Tg-AD mice. This analysis revealed that in WT mice, HDAC4 co-immunoprecipitated with several postsynaptic proteins such as the GluA1 subunit of AMPA receptor (AMPA), the postsynaptic density protein 95 (PSD95) and CaMKII (Figure 1A). In the AD hippocampal extracts, the amount and association of HDAC4 with GluA1, PSD95 and CaMKII were significantly reduced (fold changes AD vs WT: GluA1/HDAC4, 0.73 \pm 0.07, *p* < 0.01, *t* test; PSD95/HDAC4, 0.69 \pm 0.06, *p* < 0.05, *t* test; CaMKII/HDAC4, 0.61 \pm 0.18, *p* < 0.05, Mann-Whitney rank-sum test; *n* = 4; Figure 1A,B). Of note,

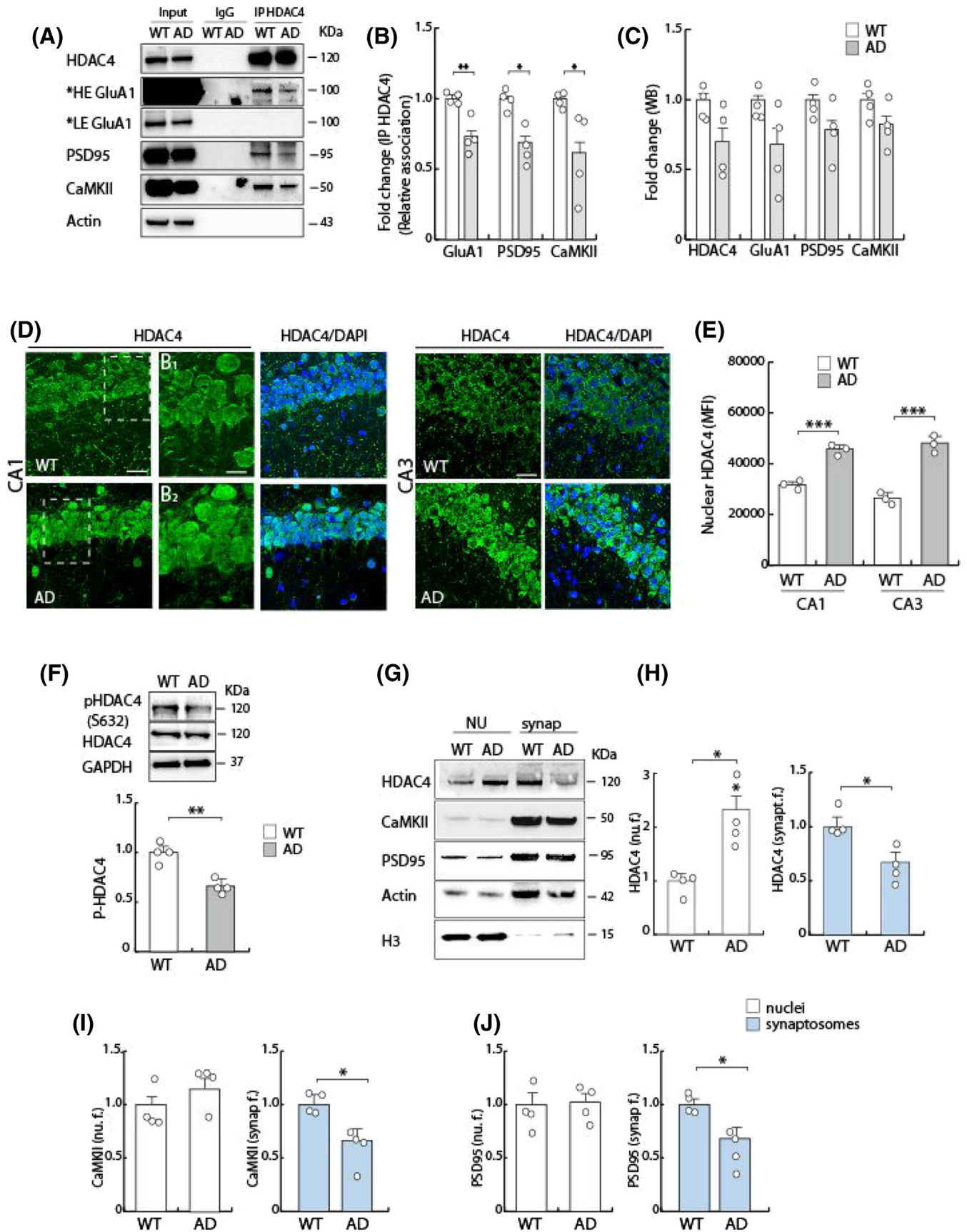


FIGURE 1 Legend on next page.

FIGURE 1 HDAC4 is delocalised from the synaptosomal compartment in AD mice. (A) Representative co-IP experiment showing HDAC4 interaction with synaptic proteins in WT and AD cytoplasmic hippocampal tissues. HE, high exposure; LE, low exposure. (B, C) Band density analysis of the relative interaction between HDAC4 and GluA1, PSD95 and CaMKII and of the levels of these proteins normalised to actin ($n = 4$). (D) Representative images showing HDAC4 localisation in hippocampal regions (CA1 and CA3) from WT and AD mice (scale bar 10 μm). Nuclei were counterstained with DAPI. (B₁, B₂) Higher magnification images are shown in the insets (scale bar 5 μm). (E) Graph showing the HDAC4 mean fluorescence intensity measured in the nuclei from the two regions of WT and AD mice ($n = 3$ mice). (F) Western blotting analysis of total and p-HDAC4 (S632) in WT and AD mice. The graph shows the densitometric analysis of p-HDAC4 normalised to GAPDH loading control and total HDAC4 content ($n = 4$ mice). (G, H) Cellular fractionation showing HDAC4 distribution in the nuclear (nu.f.) and synaptosomal compartments (synapt.f.) in extracts from WT and AD mice and their densitometric analyses ($n = 4$ mice). (I, J) Quantification of CaMKII and PSD95 in the two fractions relative to actin loading control. CaMKII, PSD95, actin and H3 expression were used as controls for fraction purity and separation. * $p < 0.05$; *** $p < 0.001$ vs WT

the protein levels of the synaptic proteins analysed by WB showed a decreasing trend that was not statistically significant (HDAC4, $p = 0.115$, Mann–Whitney rank-sum test; GluA1, $p = 0.114$, t test; PSD95, $p = 0.119$, t test; CaMKII, $p = 0.124$, Mann–Whitney rank-sum test; $n = 4$; Figure 1C). To test whether the decreased HDAC4/synaptic target interaction depended on its delocalisation from the synaptic compartment and sequestration into the nucleus, we analysed HDAC4 localisation in the CA3–CA1 hippocampal regions by confocal microscopy. In WT brain sections, HDAC4 was mainly localised in the projections and outside the nucleus, whereas it accumulated in the nuclei of the CA1 and CA3 hippocampal neurons of AD mice (Figure 1D,E) as indicated by the semi-quantitative analysis of MFI (MFI CA1: WT $31,717.42 \pm 503.43$, AD $45,876.88 \pm 896.68$; MFI CA3: WT $26,461.02 \pm 1049.66$, AD $48,118.13 \pm 2003.9$; $p < 0.001$, ANOVA with Bonferroni's test; $n = 3$).

Because HDAC4 cytoplasmic retention is positively regulated by phosphorylation, we analysed by WB possible changes in the level of p-HDAC4 (S632) in tissues from WT and AD mice. We found that p-HDAC4 levels were significantly reduced in AD extracts when compared with WT lysates (fold decrease AD vs WT: 0.66 ± 0.04 , $p < 0.01$, t test; $n = 4$; Figure 1F).

Because CaMKII phosphorylates HDAC4 and promotes its nuclear export and localisation in the cytoplasm [8], we reasoned that lower levels of p-HDAC4 could be due to reduced activation of CaMKII. We found that the level of p-Thr286-CaMKII, used as a readout of its activation, was diminished in AD tissue compared with WT one (fold change AD vs WT: 0.39 ± 0.049 , $p < 0.001$, t test; $n = 3$; Figure S1A). Furthermore, treatment of hippocampal neurons with synaptotoxic concentrations of human synthetic A β (200 μM) or recombinant human tau 2N/4R (100 nM) [30, 31] for 24 h also reduced p-CaMKII levels indicating the contribution of the two AD hallmarks to CaMKII inhibition (p-CaMKII fold change vs control: A β , 0.65 ± 0.10 , $p < 0.05$; tau, 0.44 ± 0.06 , $p < 0.01$, ANOVA with Bonferroni's test; $n = 3$; Figure S1B).

Other important players in the cytoplasmic retention of HDAC4 are the 14-3-3 proteins, a family that acts as adaptor or anchoring proteins. 14-3-3 β and ϵ have been reported as HDAC4 regulators. These proteins bind to the serine phospho-sites and retain phosphorylated HDAC4 in the cytoplasm [36, 37]. As expected, in total extracts, the pan-antibody for 14-3-3 detected several isoforms running between 28 and 30 kDa in both WT and AD extracts

(Figure S1C). Co-IP experiments showed that, in agreement with reduced p-HDAC4 levels in AD tissue and HDAC4 nuclear import, the interaction between HDAC4 and the faster running isoforms of 14-3-3 (possibly 14-3-3 β and ϵ) was reduced (fold change AD vs WT: HDAC4/14-3-3, 0.64 ± 0.07 , $p < 0.05$, t test; $n = 3$; Figure S1C).

To further characterise the presence of HDAC4 at the synapse, we performed biochemical fractionation tests. This assay revealed a substantial decrease in HDAC4 levels in the synaptosomal fraction of AD animals compared to WT mice (fold decrease AD vs WT: 0.62 ± 0.08 , $p < 0.05$, Mann–Whitney rank-sum test; $n = 4$; Figure 1G,H) that was paralleled by an enrichment of HDAC4 in the nuclei of AD mice (fold increase AD vs WT: 2.14 ± 0.36 , $p < 0.05$, t test; $n = 4$), thus confirming HDAC4 subcellular delocalisation in AD. Immunoblotting with CaMKII, actin, PSD95 and histone H3 were used as markers of the synaptosomal and nuclear fractions, respectively. Moreover, quantification of CaMKII and PSD95 protein levels revealed that their amount in the synaptosomal fraction was reduced (fold decrease AD vs WT: CaMKII, 0.66 ± 0.11 ; PSD95, 0.68 ± 0.12 ; $p < 0.05$, t test; $n = 4$), whereas protein levels were unchanged in the nuclear fraction (Figure 1I,J). We also treated cultured hippocampal neurons from WT mice with A β or tau for 24 h to determine the contribution of these species to HDAC4 delocalisation. Confocal analyses showed that either A β or tau treatments induced HDAC4 nuclear accumulation (MFI: CTRL $41,816 \pm 3477$; A β $68,311 \pm 2332$; tau $69,041 \pm 1193$, $p < 0.001$, ANOVA with Bonferroni's test, $n = 5$; Figure 2A,B) that was paralleled by a decrease in HDAC4 fluorescence intensity at the level of dendrites (MFI: CTRL 6452.79 ± 710.87 ; A β 2434.33 ± 140.88 ; tau 1946.91 ± 206.70 , $p < 0.01$, $p < 0.001$, ANOVA with Bonferroni's test; $n = 3$; Figure 2C,D).

Biochemical fractionation of neuronal cultures showed that HDAC4 synaptosomal localisation in control cells was lost in favour of a nuclear import in A β - or tau-treated cells (fold decrease treatment vs control, synapt.f.: A β , 0.75 ± 0.05 ; tau, 0.54 ± 0.09 , ANOVA with Bonferroni's test, $n = 4$; fold increase nu.f.: A β , 1.43 ± 0.11 ; tau, 1.53 ± 0.13 , $p < 0.05$ for all comparisons, ANOVA on ranks with Student–Newman–Keuls' test; $n = 4$; Figure 2E,F).

Next, we investigated whether a direct interaction of HDAC4 with A β or tau occurred in extracts from WT and AD mice. Co-IP analysis showed a binding between HDAC4 and A β only in extracts from AD mice (Figure 2G), suggesting a potential negative effect of A β on HDAC4 localisation and function. Analysis of the interaction of

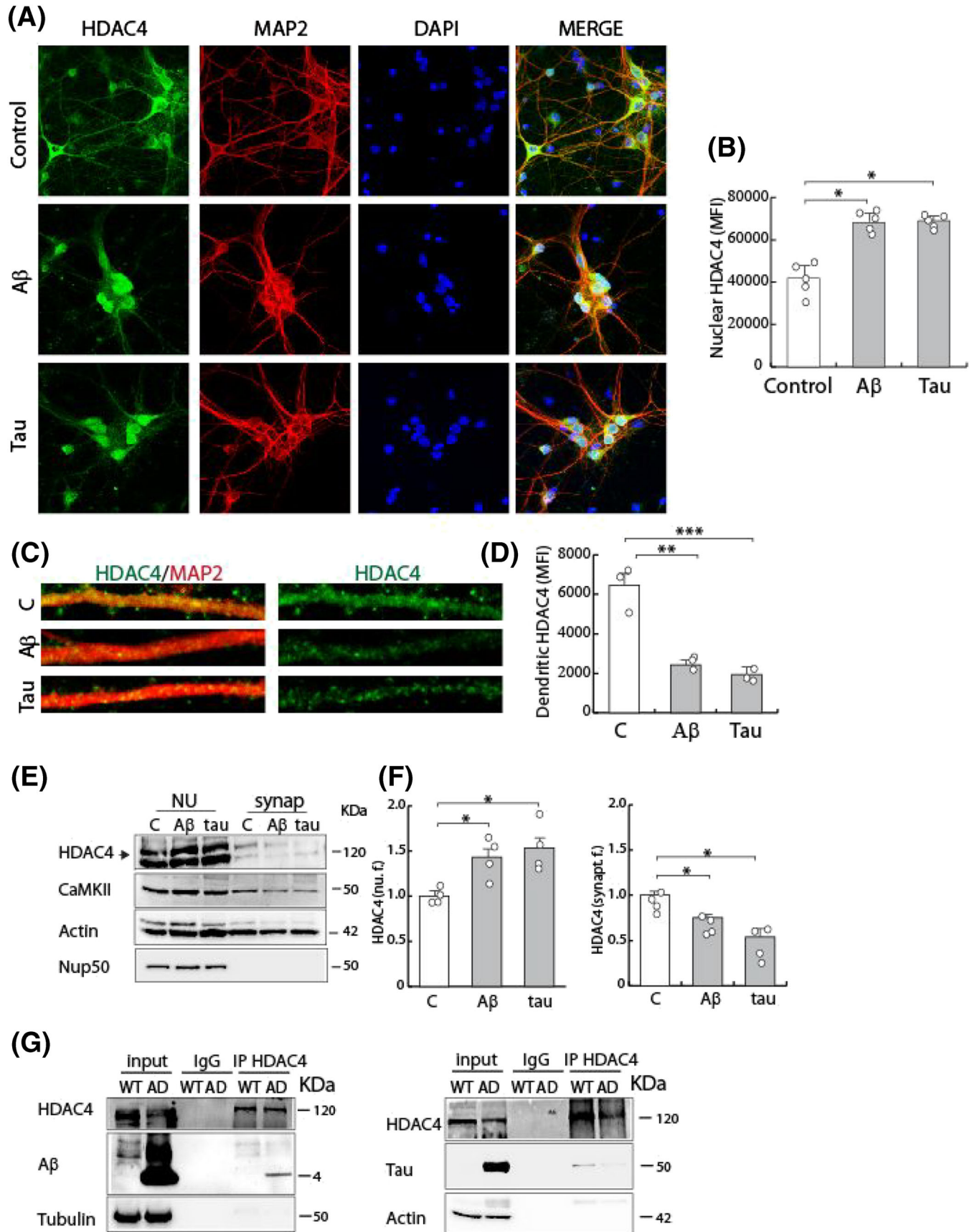


FIGURE 2 Legend on next page.

FIGURE 2 Role of A β and tau in HDAC4 delocalisation. (A) HDAC4 distribution was analysed by confocal analysis in MAP2⁺ hippocampal neurons treated for 24 h with A β or tau (scale bar 20 μ m). (B) The graph shows the mean fluorescence intensity (MFI) for nuclear HDAC4 ($n = 5$ preparations). (C, D) Evaluation of HDAC4 mean fluorescence intensity in MAP2⁺ dendrites in the above conditions ($n = 3$). (E, F) Cellular fractionation showing HDAC4 distribution in the nuclear and the synaptosomal compartments in extracts from WT cultured neurons treated with A β or tau for 24 h (a non-specific band for HDAC4 was also present in the WB). (F) Densitometric analysis of HDAC4 distribution in the two fractions ($n = 4$ preparations). CaMKII, actin and Nup50 were used as controls for fraction separation and Nup50 and actin for nuclear and synaptosomal normalisation, respectively. (G) Representative images of co-IPs showing the association between HDAC4 and A β or tau in WT and AD extracts ($n = 3$). * $p < 0.05$ vs control. Equal loading between samples is indicated by similar levels of tubulin or actin.

HDAC4 and tau revealed no specific binding between the two proteins in AD extracts.

The cytoplasmic form of HDAC4 promotes protein localisation at the postsynapse in AD neurons

Misplacement of HDAC4 from synapses could affect protein proper localisation/anchoring to the membrane and/or their function. To investigate the role of cytoplasmic HDAC4, we overexpressed an HDAC4 phosphomimetic mutant with cytoplasmically restricted localisation deriving from the substitution of serine in positions 246 and 632 with aspartic acid (HDAC4^{SD}). This construct was validated in the SH-SY5Y human neuroblastoma cell line, which does not express endogenous HDAC4. Thus, the HDAC4^{SD} or the HDAC4^{WT} constructs were overexpressed in SH-SY5Y, which then were treated for 24 h with A β and tau. Although HDAC4^{WT} was primarily localised in the cytoplasm but accumulated in the nucleus after A β and tau treatments, HDAC4^{SD} mutant was localised in the cytoplasm and its localisation was unaffected by A β or tau treatments (Figure S2A–D).

Cultured hippocampal neurons were transduced with the HDAC4^{SD} mutant (AD) or the GFP control vector (WT and AD) at DIV3 (Figure S2E). Morphological analysis performed at DIV14 by IF staining against the neuronal marker MAP2 revealed that WT-GFP neurons exhibited longer dendrites than AD-GFP neurons (Figure 3A). Of note, overexpression of HDAC4^{SD} in AD neurons recovered dendritic length to control values (WT-GFP 122.63 \pm 5.72 μ m, AD-GFP 75.21 \pm 3.38 μ m, AD-SD 112.92 \pm 4.53 μ m, $p < 0.001$, AD-GFP vs AD-SD, ANOVA with Bonferroni's test; $n = 5$), suggesting structural changes (Figure 3A,B).

Thus, we first addressed the potential role of cytoplasmic HDAC4 in providing a scaffold for proper protein localisation by analysing the presence of several postsynaptic proteins in the synaptosomal fractions isolated from DIV14 AD neuronal cultures transduced with lentiviruses coding for HDAC4^{SD} or a control vector. Overexpression of HDAC4^{SD} in AD neurons was associated with an enrichment of N-cadherin (NCAD), GluA1, PSD95 and CaMKII compared with AD control cells (fold increase: HDAC4, 5.17 \pm 0.83; NCAD, 2.25 \pm 0.46; GluA1, 1.59 \pm 0.13; PSD95, 2.19 \pm 0.18; CaMKII, 1.61 \pm 0.19; $p < 0.05$, $p < 0.01$, ANOVA with Bonferroni's test; $n = 4$; Figure 3C). Of note, the recovery of postsynaptic proteins in AD-SD transduced neurons, at the level of the synapse, was similar to WT neurons

(no significant differences between WT and AD-SD in protein level for CaMKII, PSD95, GluA1, ANOVA on ranks with Student-Newman-Keuls' test; $n = 4$; Figure S4). To test the involvement of the HDAC4 deacetylase activity in protein localisation, we analysed the synaptosomal protein content in WT hippocampal neurons treated with the HDAC4-specific inhibitor LMK-235 (40 μ M) for 24 h.

Reduction of deacetylase activity was monitored by measuring the level of total acetylated proteins that were increased in LMK-treated neurons (fold increase vs control: acetyllysine, 2.93 \pm 0.77, $p < 0.05$, ANOVA with Bonferroni's test; $n = 4$; Figure 3D). However, no significant changes were found in the levels of PSD95, GluA1 and CaMKII in the synaptosomes between WT neurons untreated or treated with LMK-235 (Figure 3D), suggesting that HDAC4-dependent deacetylation may not be the main mechanism responsible for the synaptic localisation of these proteins. Because HDAC4 may regulate other PTM such as SUMOylation [23], we investigated the SUMO2/3ylation level of PSD95, a key protein at the postsynapse, by the in vitro SUMOylation assay in WT and AD tissues. We found that the SUMO2/3-PSD95 level was diminished in extracts from AD mice (fold decrease vs WT: 0.35 \pm 0.05, $p < 0.001$, ANOVA with Bonferroni's test; $n = 3$; Figure 3E). The involvement of HDAC4 in the regulation of PSD95 SUMO2/3ylation was confirmed by repeating the in vitro SUMOylation assay in WT and AD extracts in the absence or in the presence of HDAC4^{SD} or IgG purified by IP as control. The level of SUMO2/3-PSD95, which was reduced in AD extracts compared with WT extracts, was recovered by the addition of HDAC4^{SD} (fold change SUMO2/3-PSD95: AD, 0.46 \pm 0.02; AD-SD, 1.28 \pm 0.19, $p < 0.05$, ANOVA with Bonferroni's test; $n = 3$; Figure 3F).

To understand whether the enrichment of postsynaptic proteins due to HDAC4^{SD} expression positively impacted structural changes at dendritic spines, we used organotypic hippocampal slice cultures obtained from WT or AD mice that maintain the hippocampal architecture. These slices were cultured on porous membranes for 2 weeks to allow accumulation of the AD markers A β and tau in samples isolated from 3 \times Tg-AD mice (fold increase AD vs WT: A β , 16.56 \pm 2.74, $p < 0.05$, ANOVA on ranks with Dunn's test; $n = 5$ –6; tau, 4.02 \pm 0.32, $p < 0.001$, ANOVA with Bonferroni's test; $n = 6$ –7; Figure S2A,B). We biolistically transfected organotypic hippocampal slice cultures with a DsRed plasmid, for stable whole-cell labelling and morphological analysis, alone (WT and AD) or in combination with HDAC4^{SD} (AD) to analyse spine density by confocal microscopy. The number of spines measured in AD neurons was significantly lower than in WT cells, but it was recovered by the overexpression of

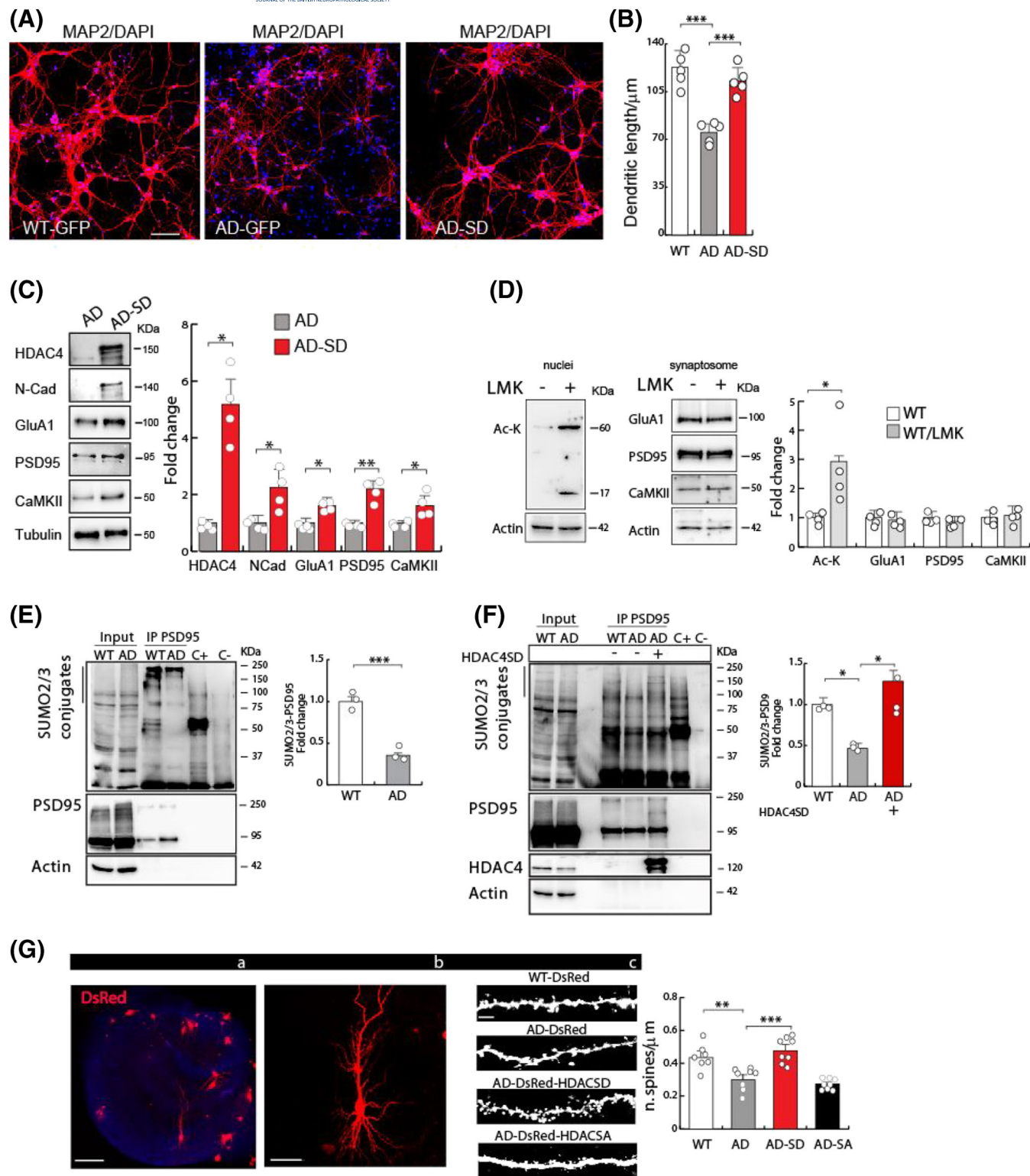


FIGURE 3 Legend on next page.

FIGURE 3 HDAC4 cytoplasmic mutant recovers synaptic protein localisation and spine density in AD mice. (A) Representative confocal images showing WT-GFP, AD-GFP and AD-SD cultured neurons (transduced with HDAC4^{SD} or the GFP control vectors) labelled with MAP2 antibody. Nuclei were stained with DAPI (scale bar 25 μ m). (B) The graph shows the analysis of dendritic length in WT, AD and AD-HDAC4^{SD}-transduced neurons at DIV14 ($n = 5$ preparations). (C) Evaluation of protein content (HDAC4, CaMKII, PSD95, N-cadherin and GluA1) in the synaptosomal fraction isolated from AD neurons transduced with HDAC4^{SD} or control lentiviruses. The graph shows the densitometric analysis ($n = 4$ preparations), and tubulin was used as the loading control. (D) Analysis of PSD95, GluA1 and CaMKII protein levels in the synaptosomes isolated from WT neurons untreated and treated with the HDAC4 inhibitor LMK235. Acetylation of histone H3 at lysine 14 was used as a readout of LMK235 activity. Densitometry is shown on the right ($n = 4$ preparations), and actin was used as the loading control. (E) Evaluation of SUMO2/3-PSD95 level in WT and AD hippocampal tissues. The relative amount of SUMO2/3-PSD95 is shown in the graph ($n = 3$ mice) and was normalised vs the immunoprecipitated total PSD95. (F) In vitro analysis of SUMO2/3-PSD95 level in AD extracts in the presence of purified IgG or GFP-HDAC4^{SD} compared with WT extracts. Densitometry is shown in the graph ($n = 3$ mice). SUMO-RanGAP was used as a positive control of the enzymatic reaction, whereas the negative control was run without the target protein and the Mg-ATP co-factor. (G) Representative images of organotypic hippocampal slice culture (a) and a CA1 neuron (b) analysed for spine density after transfection by Gene Gun with plasmids to express DsRed alone or in combination with Flag-HDAC4^{SD} or Flag-HDAC4^{SA} (scale bar 250 and 100 μ m). Red fluorescence identifies transfected neurons. (c) Right panels show representative dendrites and the assessment of spine density in WT, AD, AD-HDAC4^{SD}- and AD-HDAC4^{SA}-transfected organotypic slices ($n = 7$ –8 neurons for each experimental condition; scale bar 5 μ m). * $p < 0.05$, ** $p < 0.01$ and *** $p < 0.001$

HDAC4^{SD} (fold change spine/ μ m: WT, 0.43 ± 0.03 ; AD control, 0.29 ± 0.02 ; AD-HDAC4^{SD}, 0.48 ± 0.03 , $p < 0.05$, $p < 0.001$, ANOVA with Bonferroni's test; $n = 7$ –8 neurons; Figure 3G). As a further control, we transfected AD organotypic hippocampal slices with the HDAC4^{SA} mutant (serine 246/S632 substitution to alanine 246/A632) that cannot be phosphorylated and shows a prevalent nuclear localisation (Figure S2A–D). In this condition, we did not observe an additional decrease of spine density compared with AD control neurons (fold change spine/ μ m: AD control, 0.29 ± 0.02 ; AD-HDAC4^{SA}, 0.27 ± 0.02 , ANOVA with Bonferroni's test; $n = 8$ neurons; Figure 3G).

Functional recovery induced by the cytoplasmic form of HDAC4 in AD organotypic slices

Our data suggest that HDAC4^{SD} expression in hippocampal neurons from AD mice may restore synaptic function. To corroborate these findings, we next compared basal synaptic transmission at CA3–CA1 glutamatergic synapses in organotypic hippocampal slices from WT and AD mice transfected with DsRed alone or in combination with HDAC4^{SD}. To this aim, we performed patch-clamp (whole-cell configuration) recordings of synaptic currents in DsRed-expressing CA1 pyramidal neurons and optimised the electrical stimulation of Schaffer collaterals to estimate AMPAR-mediated EPSCs evoked by different stimulus intensities. The input–output relationship of AMPAR-mediated EPSCs in HDAC4^{SD}-transfected neurons was significantly increased as compared with those recorded in DsRed-transfected neurons (current stimulation 300 μ A: AD-SD, 2.14 ± 0.42 nA, $n = 12$; AD, 1.05 ± 0.26 nA, $n = 10$, one-way ANOVA, $F_{(2, 22)} = 4.64$; followed by Dunn's post hoc test, $p < 0.05$; Figure 4A). Noteworthy, EPSC amplitudes in AD neurons overexpressing HDAC4^{SD} were similar to those recorded in CA1 neurons from WT mice (current stimulation 300 μ A: WT, 1.80 ± 0.32 nA, $n = 13$, one-way ANOVA, $F_{(2, 25)} = 0.5$; followed by Dunn's post hoc test, $p > 0.05$). To test whether the increased AMPAR-mediated EPSCs in HDAC4^{SD}-transfected neurons were mediated by a postsynaptic mechanism, we

studied the PPF. No significant differences in PPF ratio were found between DsRed- and HDAC4^{SD}-transfected AD neurons (one-way ANOVA, $F_{(2, 26)} = 0.7$; followed by Dunn's post hoc test, $p > 0.05$; Figure 4B).

We also examined mEPSCs in HDAC4^{SD}- and DsRed-transfected AD neurons and found a significant difference in their amplitude (26.2 ± 2.2 vs 19.0 ± 0.9 pA; one-way ANOVA, $F_{(2, 28)} = 9.6$; followed by Dunn's post hoc test, $p < 0.05$; $n = 14$ for both groups; Figure 4C,D). Instead, the mEPSC rise time, decay time and frequency showed no significant differences (rise time: 1.05 ± 0.05 vs 1.07 ± 0.11 ms; one-way ANOVA, $F_{(2, 28)} = 0.2$; followed by Dunn's post hoc test, $p > 0.05$; decay time: 6.2 ± 0.2 vs 4.9 ± 0.4 ms; one-way ANOVA, $F_{(2, 28)} = 0.1$; followed by Dunn's post hoc test, $p > 0.05$; frequency: 0.32 ± 0.03 vs 0.33 ± 0.06 Hz; one-way ANOVA, $F_{(2, 28)} = 0.2$; followed by Dunn's post hoc test, $p < 0.05$; $n = 14$ for both groups; Figure 4C–G). Collectively, these findings suggest that HDAC4^{SD} expression in hippocampal neurons from AD mice restores glutamatergic synaptic transmission that was impaired at the postsynaptic level.

DISCUSSION

In this study, we investigated the role of the cytoplasmic HDAC4 pool in the postsynaptic compartment under physiological conditions and in the 3 \times Tg mouse model of AD.

We found that HDAC4 localisation at the synapse and its interaction with synaptic proteins were significantly reduced in AD mice that exhibited HDAC4 accumulation in the nucleus. Amyloid- β and tau were found to contribute, at least in part, to HDAC4 delocalisation in neurons. Overexpression of a cytoplasmically restricted mutant form of HDAC4 in AD neurons induced (i) enrichment of synaptic proteins, (ii) recovery of spine density, (iii) dendrite elongation and (iv) ameliorated synaptic transmission. Our results reveal a new cytoplasmic role of HDAC4, so far unexplored, and open the way for potential therapeutic approaches based on the regulation of HDAC4 localisation boosting synaptic function.

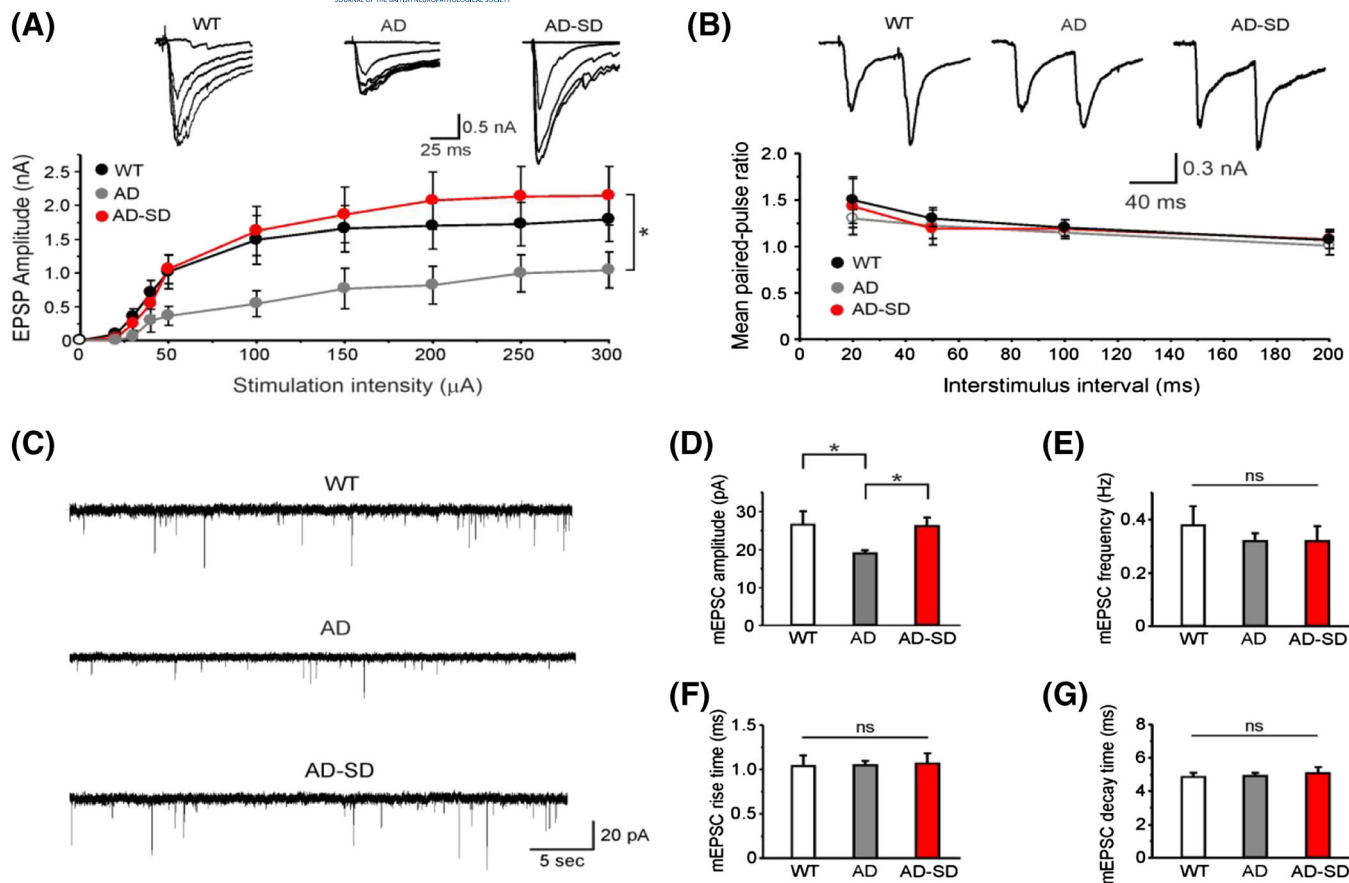


FIGURE 4 HDAC4 cytoplasmic mutant recovers synaptic function in AD mice. (A) Input–output (I–O) curve showing the average amplitudes of synaptic AMPAR-mediated currents recorded in CA1 pyramidal neurons from AD organotypic slices transfected with DsRed alone or in combination with HDAC4^{SD}. I–O curve recorded in slices from DsRed-transfected WT mice is also shown (AD, *n* = 10 neurons; AD-HDAC4^{SD}, *n* = 12 neurons; WT, *n* = 13 neurons). ANOVA revealed a significant effect of HDAC4^{SD} expression on AMPAR current amplitudes compared with AD, across stimulation intensities (*p* < 0.05). Inset: Representative traces of AMPAR-mediated currents in the different experimental conditions shown in (A). (B) Mean paired-pulse ratio values in pyramidal neurons from WT, AD and AD-HDAC4^{SD} hippocampal slices transfected with DsRed are shown for different interstimulus intervals. Note that paired-pulse ratio values were not significantly different in all the experimental conditions (AD, *n* = 12 neurons; AD-HDAC4^{SD}, *n* = 14 neurons; WT, *n* = 11 neurons). (C) Representative traces of mEPSCs recorded in organotypic CA1 pyramidal neurons from WT, AD and AD-HDAC4^{SD} slices. Mean values for mEPSC amplitude (D), frequency (E), rise time (F) and decay time (G) in the different experimental conditions. Note that a significant effect of HDAC4^{SD} expression was found only for mEPSC amplitudes (AD, *n* = 12 neurons; AD-HDAC4^{SD}, *n* = 14 neurons; WT, *n* = 11 neurons). **p* < 0.05 vs WT; #*p* < 0.05 vs AD. ‘ns’ means not significant.

Previous studies have shown that inhibition of HDAC3 or HDAC6 was beneficial for AD by improving memory and cognition [38, 39]. Mechanistically, inhibition of both HDAC3 and HDAC6 reduced A β metabolism and tau hyperphosphorylation lowering their accumulation. Our results expand knowledge of the role of HDACs in AD uncovering HDAC4 as a new player. In contrast to HDAC3 and HDAC6, whose activation negatively affects AD-related pathology, HDAC4 exerts a regulatory function at the synaptic level possibly acting as a scaffold for the different post-synaptic density proteins, thus strengthening synaptic transmission. Our findings also highlight that neurodegeneration and synaptic dysfunction in AD may derive not only from HDAC4 nuclear import and consequent plasticity-related gene repression but also from the loss of the positive function played by HDAC4 at the dendritic

spines. As such, selective HDAC4 inhibition could be only partially beneficial in the absence of the recovery of its cytoplasmic function. On the other hand, the expression of the cytoplasmic HDAC4 mutant in AD neurons ameliorated spine density and neuronal function, even in the presence of the endogenous HDAC4 protein localised in the nucleus suggesting a dominant positive effect of the HDAC4 mutant.

Looking at the possible mechanisms affecting HDAC4 delocalisation, we found that both A β and tau were able to drive HDAC4 nuclear import. In addition to the toxic extracellular action of A β , including negative signalling to synaptic dysfunction through receptor binding [40], it also accumulates intracellularly, at the level of dendrites and spines [41], where it can interact with several proteins belonging to energy metabolism, cytoskeleton, gene expression and

signal transduction [42–44]. Although we did not investigate here the effects of A β -HDAC4 interactions, we can speculate that this binding may affect HDAC4 association with synaptic proteins and may favour its shuttling to the nucleus.

Previous work performed in *in vitro* experiments with recombinant proteins showed tau binding with several HDACs but not with HDAC4 [45]. In the present paper, we investigated the HDAC4/tau association in WT and AD tissues and found a low and not specific binding for AD. These results suggest that direct HDAC4/tau interaction may not be the main mechanism for HDAC4 alteration. In this context, the finding that in AD tissue as well as in A β - and tau-treated neurons the phosphorylation of CaMKII is reduced indicates that AD hallmarks may affect the CaMKII downstream signalling to HDAC4. Indeed, CaMKII-dependent phosphorylation of HDAC4 promotes its nuclear export and retention in the cytoplasm [8]. Thus, the reduction of CaMKII activation (i.e., its reduced phosphorylation) in AD tissue, possibly due to the toxic effect of A β and tau, may be responsible for the lower p-HDAC4 levels that we found in AD tissues. Consequently, the binding of the anchoring protein 14-3-3 to the HDAC4 serine phospho-sites is affected in AD and concurs with HDAC4 delocalisation.

One of the earliest features of AD is dendritic spine loss and consequent reduction of spine density that correlates with functional impairment. Dendritic spines include several functionally distinct microdomains that ensure efficient changes in spine structure and function. For example, PSD, which also receives direct signals from the presynaptic termini, consists of a submembranous protein mesh that gathers scaffolding factors, signalling molecules and cytoskeletal proteins.

We found that HDAC4 is part of this network and exerts a scaffolding action allowing the enrichment and localisation of several proteins at synapses. Indeed, its cytoplasmic-restricted mutant overexpressed in these specific microdomains promoted, in AD neurons, the enrichment of PSD95, GluA1, CaMKII and NCAD, all proteins important for synapse structure and function. These data were paralleled by the recovery of spine density in AD neurons after HDAC4^{SD} overexpression suggesting an important structural role for HDAC4. Of note, accumulation of PSD95 is required for spine stabilisation [46], and both PSD95 and CaMKII promote the stabilisation of young synapses [47]. NCAD, which we also found enriched after HDAC4^{SD} overexpression, is an integral membrane protein that ensures the adhesion between synaptic membranes interacting with actin. Recent studies have highlighted that synaptic adhesion molecules regulate synapse development and maintenance at different steps facilitating the contact between the presynaptic and postsynaptic termini, promoting the formation of young synapses and providing stability and maturation of synapses [48].

CaMKII is one of the key players at the PSD implicated in synaptic transmission and activity-dependent processes and plasticity [49]. Among the numerous effects, it exerts at the glutamatergic synapses

and regulates phosphorylation of AMPA receptors [50, 51], as well as their insertion and anchoring to the membrane [52, 53].

In our experiments, the accumulation of PSD95 and CaMKII was paralleled by the increase of the AMPAR subunit GluA1. Electrophysiological data showing increased EPSCs in HDAC4^{SD}-transfected AD neurons are in agreement with enhanced AMPA receptors at the postsynaptic level. Thus, the HDAC4-dependent recovery of key functional proteins at the postsynapse could be the basis of the restoration of synaptic function at CA3–CA1 synapses that we observed in organotypic slices from 3 \times Tg-AD mice. Nevertheless, we cannot exclude any effects of HDAC4 at the presynaptic compartment that were not specifically investigated in the present work.

Previous studies have shown that HDAC4 has a SUMO E3 ligase activity, which is dependent on its cytoplasmic localisation and determines protein stability or activity of its targets (e.g., I κ B α and MEF2) [54–57]. Other studies demonstrated that in *Drosophila*, HDAC4 regulates memory formation and long-term memory (LTM) induction through the interaction with the SUMO-conjugating enzyme Ubc9 [58], and its nuclear accumulation impairs neuronal development and LTM [59]. Based on these findings, we investigated the role of HDAC4 in the regulation of synaptic protein SUMOylation analysing the modification of PSD95, the key scaffold molecule at the synapse that has been recently shown to colocalise with SUMO2/3 and Ubc9 in hippocampal neurons [60]. Our results suggest that in addition to a structural role, HDAC4 may promote synaptic protein function and localisation through their SUMOylation. Indeed, because SUMO and ubiquitin may modify the same acceptor lysine, SUMO modification can prevent ubiquitination and protein targeting to degradation favouring protein stabilisation and accumulation at the synapse. Whether HDAC4 may serve as an E3 SUMOylation enzyme for other synaptic proteins is to date unknown. Because the SUMOylation/deSUMOylation balance is increasingly considered crucial in synaptic protein regulation and AD pathophysiology, the potential role of HDAC4 in this process represents an important field of research that deserves further investigation.

Overall, our findings indicate that a pool of HDAC4 is localised at the dendritic spines and controls postsynaptic proteins providing a scaffolding platform for proper membrane localisation and function, thus favouring spine formation and stabilisation (Figure 5A). This function is altered in AD mice due to HDAC4 delocalisation (Figure 5B). This anchoring role of cytoplasmic HDAC4 is based on a structural function and may require a deacetylase-independent function.

Although the accumulation of extracellular amyloid plaques, a hallmark of AD, does not correlate with the severity of the disease, structural injury involving abnormal spine morphology, decreased spine density and reduced levels of synaptic proteins well correlates with soluble A β oligomer accumulation [61] and with changes in tau PTMs [62]. Our data show that synaptic deterioration may indeed derive from the toxic effect of A β and tau on HDAC4 localisation

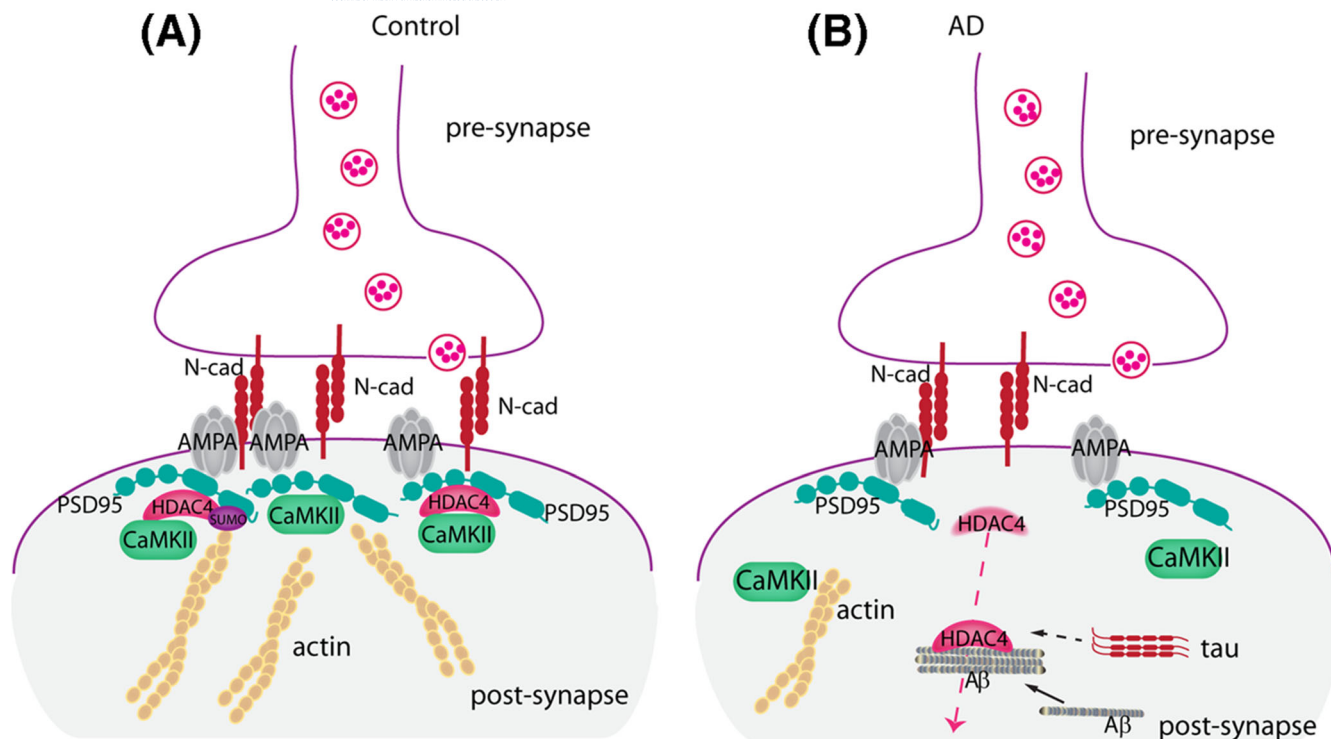


FIGURE 5 Cartoon illustrating the potential HDAC4 role at synapses. (A) Under physiological conditions, HDAC4 is localised at the dendritic spines and positively controls synaptic proteins by SUMOylation and providing a scaffolding platform for proper membrane localisation and function, thus favouring spine formation and stabilisation. (B) In AD neurons, A β - and tau-dependent mechanisms decrease HDAC4 localisation at synapses contributing to synaptic protein dysfunction and impaired synaptic transmission.

(Figure 5B). Although further studies will be required to thoroughly investigate the role of HDAC4 on synaptic function, our results indicate that recovery of HDAC4 proper localisation and function may preserve a healthy and strong neuronal network, thus protecting synapses from the negative effect of A β and tau in AD.

ACKNOWLEDGEMENTS

We acknowledge the contribution of the Core Facility G-SteP 'Electrophysiology' and the financial support of 'Ricerca Corrente 2022' from Fondazione Policlinico Universitario Agostino Gemelli IRCCS to CG. This work was partially supported by the Alzheimer's Association Research Grant (AARG) 19 614919 to CC. Open access funding provided by BIBLIOSAN.

CONFLICTS OF INTEREST

The authors declare no conflicts of interest.

ETHICS STATEMENT

All animal procedures were approved by the Ethical Committee of the Università Cattolica del Sacro Cuore and were fully compliant with the Italian (Ministry of Health guidelines, Legislative Decree No. 116/1992) and European Union (Directive No. 86/609/EEC) legislation on animal research.

AUTHOR CONTRIBUTIONS

Electrophysiology: MD, GA. Mutant generation: CR. Confocal analysis: CC, EP, WB, IP, SUMOylation assay: CC, AB, DDLP. Conceptualization: CC, CG. Writing: CC, CG. All authors read and approved the final manuscript.

PEER REVIEW

The peer review history for this article is available at <https://publons.com/publon/10.1111/nan.12861>.

DATA AVAILABILITY STATEMENT

Data published in this manuscript are available from the corresponding author upon reasonable request.

ORCID

Claudia Colussi  <https://orcid.org/0000-0002-7727-8911>

REFERENCES

1. Caselli RJ, Beach TG, Yaari R, Reiman EM. Alzheimer's disease a century later. *J Clin Psychiatry*. 2006;67(11):1784-1800. doi:10.4088/JCP.v67n1118
2. Tanzi RE. The genetics of Alzheimer disease. *Cold Spring Harb Perspect Med*. 2012;2(10):a006296. doi:10.1101/cshperspect.a006296

3. Scheltens P, De Strooper B, Kivipelto M, et al. Alzheimer's disease. *Lancet*. 2021;397(10284):1577-1590. doi:10.1016/S0140-6736(20)32205-4
4. Wegmann S, Biernat J, Mandelkow E. A current view on tau protein phosphorylation in Alzheimer's disease. *Curr Opin Neurobiol*. 2021; 69:131-138. doi:10.1016/j.conb.2021.03.003
5. Malmberg M, Malm T, Gustafsson O, et al. Disentangling the amyloid pathways: a mechanistic approach to etiology. *Front Neurosci*. 2020; 14:256. doi:10.3389/fnins.2020.00256
6. Sheng M, Sabatini BL, Sudhof TC. Synapses and Alzheimer's disease. *Cold Spring Harb Perspect Biol*. 2012;4(5):a005777. doi:10.1101/cshperspect.a005777
7. Park SY, Kim JS. A short guide to histone deacetylases including recent progress on class II enzymes. *Exp Mol Med*. 2020;52(2):204-212. doi:10.1038/s12276-020-0382-4
8. Backs J, Song K, Bezprozvannaya S, Chang S, Olson EN. CaM kinase II selectively signals to histone deacetylase 4 during cardiomyocyte hypertrophy. *J Clin Invest*. 2006;116(7):1853-1864. doi:10.1172/JCI27438
9. Chawla S, Vanhoutte P, Arnold FJ, Huang CLH, Bading H. Neuronal activity-dependent nucleocytoplasmic shuttling of HDAC4 and HDAC5. *J Neurochem*. 2003;85(1):151-159. doi:10.1046/j.1471-4159.2003.01648.x
10. Paroni G, Cernotta N, dello Russo C, et al. PP2A regulates HDAC4 nuclear import. *Mol Biol Cell*. 2008;19(2):655-667. doi:10.1091/mbc.e07-06-0623
11. Chen B, Cepko CL. HDAC4 regulates neuronal survival in normal and diseased retinas. *Science*. 2009;323(5911):256-259. doi:10.1126/science.1166226
12. Kim MS, Akhtar MW, Adachi M, et al. An essential role for histone deacetylase 4 in synaptic plasticity and memory formation. *J Neurosci*. 2012;32(32):10879-10886. doi:10.1523/JNEUROSCI.2089-12.2012
13. Sando R 3rd, Gounko N, Pieraut S, Liao L, Yates J III, Maximov A. HDAC4 governs a transcriptional program essential for synaptic plasticity and memory. *Cell*. 2012;151(4):821-834. doi:10.1016/j.cell.2012.09.037
14. Zhu Y, Huang M, Bushong E, et al. Class IIa HDACs regulate learning and memory through dynamic experience-dependent repression of transcription. *Nat Commun*. 2019;10(1):3469. doi:10.1038/s41467-019-11409-0
15. Wu Y, Hou F, Wang X, Kong Q, Han X, Bai B. Aberrant expression of histone deacetylases 4 in cognitive disorders: molecular mechanisms and a potential target. *Front Mol Neurosci*. 2016;9:114. doi:10.3389/fnmol.2016.00114
16. Lang C, Campbell KR, Ryan BJ, et al. Single-cell sequencing of iPSC-dopamine neurons reconstructs disease progression and identifies HDAC4 as a regulator of Parkinson cell phenotypes. *Cell Stem Cell*. 2019;24(1):93-106.e6. doi:10.1016/j.stem.2018.10.023
17. Trazzi S, Fuchs C, Viggiano R, et al. HDAC4: a key factor underlying brain developmental alterations in CDKL5 disorder. *Hum Mol Genet*. 2016;25(18):3887-3907. doi:10.1093/hmg/ddw231
18. Sen A, Nelson TJ, Alkon DL. ApoE4 and A β oligomers reduce BDNF expression via HDAC nuclear translocation. *J Neurosci*. 2015;35(19):7538-7551. doi:10.1523/JNEUROSCI.0260-15.2015
19. Shen X, Chen J, Li J, Kofler J, Herrup K. Neurons in vulnerable regions of the Alzheimer's disease brain display reduced ATM signaling. *eNeuro*. 2016;3(1):ENEURO.0124. doi:10.1523/ENEURO.0124-15.2016
20. Lahm A, Paolini C, Pallaoro M, et al. Unraveling the hidden catalytic activity of vertebrate class IIa histone deacetylases. *Proc Natl Acad Sci U S A*. 2007;104(44):17335-17340. doi:10.1073/pnas.0706487104
21. Fischle W, Dequiedt F, Hendzel MJ, et al. Enzymatic activity associated with class II HDACs is dependent on a multiprotein complex containing HDAC3 and SMRT/N-CoR. *Mol Cell*. 2002;9(1):45-57. doi:10.1016/S1097-2765(01)00429-4
22. Darcy MJ, Calvin K, Cavnar K, Ouimet CC. Regional and subcellular distribution of HDAC4 in mouse brain. *J Comp Neurol*. 2010;518(5):722-740. doi:10.1002/cne.22241
23. Gregoire S, Yang XJ. Association with class IIa histone deacetylases upregulates the sumoylation of MEF2 transcription factors. *Mol Cell Biol*. 2005;25(6):2273-2287. doi:10.1128/MCB.25.6.2273-2287.2005
24. Hendriks IA, Vertegaal AC. A comprehensive compilation of SUMO proteomics. *Nat Rev Mol Cell Biol*. 2016;17(9):581-595. doi:10.1038/nrm.2016.81
25. Flotho A, Melchior F. Sumoylation: a regulatory protein modification in health and disease. *Annu Rev Biochem*. 2013;82(1):357-385. doi:10.1146/annurev-biochem-061909-093311
26. Schorova L, Martin S. Sumoylation in synaptic function and dysfunction. *Front Synaptic Neurosci*. 2016;8:9. doi:10.3389/fnsyn.2016.00009
27. Nistico R, Ferraina C, Marconi V, et al. Age-related changes of protein SUMOylation balance in the A β PP Tg2576 mouse model of Alzheimer's disease. *Front Pharmacol*. 2014;5:63.
28. Li Puma DD, Marocci ME, Lazzarino G, et al. Ca²⁺-dependent release of ATP from astrocytes affects herpes simplex virus type 1 infection of neurons. *Glia*. 2021;69(1):201-215. doi:10.1002/glia.23895
29. Puzzo D, Piacentini R, Fá M, et al. LTP and memory impairment caused by extracellular A β and tau oligomers is APP-dependent. *Elife*. 2017;6:e26991. doi:10.7554/eLife.26991
30. Li Puma DD, Ripoli C, Puliatti G, et al. Extracellular tau oligomers affect extracellular glutamate handling by astrocytes through down-regulation of GLT-1 expression and impairment of NKA1A2 function. *Neuropathol Appl Neurobiol*. 2022:e12811.
31. Ripoli C, Piacentini R, Riccardi E, Li Puma DD, Bitan G, Grassi C. Effects of different amyloid β -protein analogues on synaptic function. *Neurobiol Aging*. 2013;34(4):1032-1044. doi:10.1016/j.neurobiolaging.2012.06.027
32. Renna PRC, Ripoli C, Dagliyan O, et al. Engineering a switchable single-chain TEV protease to control protein maturation in living neurons. *Bioeng Transl Med*. 2022;7(2):e10292. doi:10.1002/btm2.10292
33. Mainardi M, Spinelli M, Scala F, et al. Loss of leptin-induced modulation of hippocampal synaptic transmission and signal transduction in high-fat diet-fed mice. *Front Cell Neurosci*. 2017;11:225. doi:10.3389/fncel.2017.00225
34. Leone L, Colussi C, Gironi K, et al. Altered Nup153 expression impairs the function of cultured hippocampal neural stem cells isolated from a mouse model of Alzheimer's disease. *Mol Neurobiol*. 2019;56(8):5934-5949. doi:10.1007/s12035-018-1466-1
35. Burckhardt CJ, Minna JD, Danuser G. Co-immunoprecipitation and semi-quantitative immunoblotting for the analysis of protein-protein interactions. *STAR Protoc*. 2021;2(3):100644. doi:10.1016/j.xpro.2021.100644
36. Wang AH, Kruhlak MJ, Wu J, et al. Regulation of histone deacetylase 4 by binding of 14-3-3 proteins. *Mol Cell Biol*. 2000;20(18):6904-6912. doi:10.1128/MCB.20.18.6904-6912.2000
37. Grozinger CM, Schreiber SL. Regulation of histone deacetylase 4 and 5 and transcriptional activity by 14-3-3-dependent cellular localization. *Proc Natl Acad Sci USA*. 2000;97(14):7835-7840. doi:10.1073/pnas.140199597
38. Janczura KJ, Volmar CH, Sartor GC, et al. Inhibition of HDAC3 reverses Alzheimer's disease-related pathologies in vitro and in the 3xTg-AD mouse model. *Proc Natl Acad Sci USA*. 2018;115(47):E11148-E11157. doi:10.1073/pnas.1805436115

39. Zhang L, Liu C, Wu J, et al. Tubastatin A/ACY-1215 improves cognition in Alzheimer's disease transgenic mice. *J Alzheimers Dis*. 2014; 41(4):1193-1205. doi:10.3233/JAD-140066
40. Mucke L, Selkoe DJ. Neurotoxicity of amyloid β -protein: synaptic and network dysfunction. *Cold Spring Harb Perspect Med*. 2012;2(7): a006338. doi:10.1101/cshperspect.a006338
41. Fein JA, Sokolow S, Miller CA, et al. Co-localization of amyloid beta and tau pathology in Alzheimer's disease synaptosomes. *Am J Pathol*. 2008;172(6):1683-1692. doi:10.2353/ajpath.2008.070829
42. Medvedev AE, Buneeva OA, Kopylov AT, et al. Chemical modifications of amyloid- β (1-42) have a significant impact on the repertoire of brain amyloid- β (1-42) binding proteins. *Biochimie*. 2016;128-129: 55-58.
43. Corbacho I, Berrocal M, Török K, Mata AM, Gutierrez-Merino C. High affinity binding of amyloid β -peptide to calmodulin: structural and functional implications. *Biochem Biophys Res Commun*. 2017; 486(4):992-997. doi:10.1016/j.bbrc.2017.03.151
44. Ripoli C, Cocco S, Li Puma DD, et al. Intracellular accumulation of amyloid- β (A β) protein plays a major role in A β -induced alterations of glutamatergic synaptic transmission and plasticity. *J Neurosci*. 2014;34(38):12893-12903. doi:10.1523/JNEUROSCI.1201-14.2014
45. Trzeciakiewicz H, Ajit D, Tseng JH, et al. An HDAC6-dependent surveillance mechanism suppresses tau-mediated neurodegeneration and cognitive decline. *Nat Commun*. 2020;11(1):5522. doi:10.1038/s41467-020-19317-4
46. Ehrlich I, Klein M, Rumpel S, Malinow R. PSD-95 is required for activity-driven synapse stabilization. *Proc Natl Acad Sci U S A*. 2007; 104(10):4176-4181. doi:10.1073/pnas.0609307104
47. Taft CE, Turrigiano GG. PSD-95 promotes the stabilization of young synaptic contacts. *Philos Trans R Soc Lond B Biol Sci*. 2014;369(1633): 20130134. doi:10.1098/rstb.2013.0134
48. Jang S, Lee H, Kim E. Synaptic adhesion molecules and excitatory synaptic transmission. *Curr Opin Neurobiol*. 2017;45:45-50. doi:10.1016/j.conb.2017.03.005
49. Lisman J, Schulman H, Cline H. The molecular basis of CaMKII function in synaptic and behavioural memory. *Nat Rev Neurosci*. 2002; 3(3):175-190. doi:10.1038/nm753
50. Barria A, Derkach V, Soderling T. Identification of the Ca²⁺/calmodulin-dependent protein kinase II regulatory phosphorylation site in the α -amino-3-hydroxy-5-methyl-4-isoxazole-propionate-type glutamate receptor. *J Biol Chem*. 1997;272(52):32727-32730. doi:10.1074/jbc.272.52.32727
51. Mammen AL, Kameyama K, Roche KW, Haganir RL. Phosphorylation of the α -amino-3-hydroxy-5-methylisoxazole-4-propionic acid receptor GluR1 subunit by calcium/calmodulin-dependent kinase II. *J Biol Chem*. 1997;272(51):32528-32533. doi:10.1074/jbc.272.51.32528
52. Maletic-Savatic M, Koothan T, Malinow R. Calcium-evoked dendritic exocytosis in cultured hippocampal neurons. Part II: mediation by calcium/calmodulin-dependent protein kinase II. *J Neurosci*. 1998; 18(17):6814-6821. doi:10.1523/JNEUROSCI.18-17-06814.1998
53. Lisman JE, Zhabotinsky AM. A model of synaptic memory: a CaMKII/PP1 switch that potentiates transmission by organizing an AMPA receptor anchoring assembly. *Neuron*. 2001;31(2):191-201. doi:10.1016/S0896-6273(01)00364-6
54. Yang Q, Tang J, Xu C, et al. Histone deacetylase 4 inhibits NF- κ B activation by facilitating I κ B α sumoylation. *J Mol Cell Biol*. 2020; 12(12):933-945. doi:10.1093/jmcb/mjaa043
55. Grégoire S, Tremblay AM, Xiao L, et al. Control of MEF2 transcriptional activity by coordinated phosphorylation and sumoylation. *J Biol Chem*. 2006;281(7):4423-4433. doi:10.1074/jbc.M509471200
56. Yang Y, Tse AK, Li P, et al. Inhibition of androgen receptor activity by histone deacetylase 4 through receptor SUMOylation. *Oncogene*. 2011;30(19):2207-2218. doi:10.1038/onc.2010.600
57. Zhao X, Sternsdorf T, Bolger TA, Evans RM, Yao TP. Regulation of MEF2 by histone deacetylase 4- and SIRT1 deacetylase-mediated lysine modifications. *Mol Cell Biol*. 2005;25(19):8456-8464. doi:10.1128/MCB.25.19.8456-8464.2005
58. Schwartz S, Truglio M, Scott MJ, Fitzsimons HL. Long-term memory in *Drosophila* is influenced by histone deacetylase HDAC4 interacting with SUMO-conjugating enzyme Ubc9. *Genetics*. 2016;203(3):1249-1264. doi:10.1534/genetics.115.183194
59. Main P, Tan WJ, Wheeler D, Fitzsimons HL. Increased abundance of nuclear HDAC4 impairs neuronal development and long-term memory. *Front Mol Neurosci*. 2021;14:616642. doi:10.3389/fnmol.2021.616642
60. Colnaghi L, Russo L, Natale C, et al. Super resolution microscopy of SUMO proteins in neurons. *Front Cell Neurosci*. 2019;13:486. doi:10.3389/fncel.2019.00486
61. Terry RD, Masliah E, Salmon DP, et al. Physical basis of cognitive alterations in Alzheimer's disease: synapse loss is the major correlate of cognitive impairment. *Ann Neurol*. 1991;30(4):572-580. doi:10.1002/ana.410300410
62. Wesseling H, Mair W, Kumar M, et al. Tau PTM profiles identify patient heterogeneity and stages of Alzheimer's disease. *Cell*. 2020; 183(6):1699-1713.e13. doi:10.1016/j.cell.2020.10.029

SUPPORTING INFORMATION

Additional supporting information can be found online in the Supporting Information section at the end of this article.

How to cite this article: Colussi C, Aceto G, Ripoli C, et al. Cytoplasmic HDAC4 recovers synaptic function in the 3 \times Tg mouse model of Alzheimer's disease. *Neuropathol Appl Neurobiol*. 2023;49(1):e12861. doi:10.1111/nan.12861